Colloids and Surfaces B: Biointerfaces 130 (2015) 222–228

Contents lists available at ScienceDirect

Colloids and Surfaces B: Biointerfaces

journal homepage: www.elsevier.com/locate/colsurfb

Effect of negatively charged cellulose nanofibers on the dispersion of hydroxyapatite nanoparticles for scaffolds in bone tissue engineering

Minsung Park[a], Dajung Lee[a], Sungchul Shin[a], Jinho Hyun[a,b,c,*]

[a] Department of Biosystems and Biomaterials Science and Engineering, Seoul National University, Seoul 151-921, Republic of Korea
[b] Research Institute of Agriculture and Life Sciences, Seoul National University, Seoul 151-921, Republic of Korea
[c] Center for Food and Bioconvergence, Seoul National University, Seoul 151-921, Republic of Korea

ARTICLE INFO

Article history:
Received 19 January 2015
Received in revised form 6 April 2015
Accepted 7 April 2015
Available online 15 April 2015

Keywords:
Colloidal stability
Dispersant
Hydroxyapatite
Bacterial cellulose
Scaffold

ABSTRACT

Nanofibrous 2,2,6,6-tetramethylpiperidine-1-oxyl(TEMPO)-oxidized bacterial cellulose (TOBC) was used as a dispersant of hydroxyapatite (HA) nanoparticles in aqueous solution. The surfaces of TOBC nanofibers were negatively charged after the reaction with the TEMPO/NaBr/NaClO system at pH 10 and room temperature. HA nanoparticles were simply adsorbed on the TOBC nanofibers (HA–TOBC) and dispersed well in DI water. The well-dispersed HA–TOBC colloidal solution formed a hydrogel after the addition of gelatin, followed by crosslinking with glutaraldehyde (HA–TOBC–Gel). The chemical modification of the fiber surfaces and the colloidal stability of the dispersion solution confirmed TOBC as a promising HA dispersant. Both the Young's modulus and maximum tensile stress increased as the amount of gelatin increased due to the increased crosslinking of gelatin. In addition, the well-dispersed HA produced a denser scaffold structure resulting in the increase of the Young's modulus and maximum tensile stress. The well-developed porous structures of the HA–TOBC–Gel composites were incubated with Calvarial osteoblasts. The HA–TOBC–Gel significantly improved cell proliferation as well as cell differentiation confirming the material as a potential candidate for use in bone tissue engineering scaffolds.

1. Introduction

Hydroxyapatite ($Ca_{10}(PO_4)_6(OH)$, HA) is the natural inorganic component of hard tissues and has been used extensively for bone repair, fillers, and substitution due to its excellent biocompatibility and bioactivity. In spite of the similarity of HA to the components of real bone, HA nanoparticles are not easily dispersed; instead, they easily aggregate to form precipitates due to the inherent unstable colloidal nature of HA that makes it difficult to form a controlled structure [1–3]. Because a solution process is usually required to fabricate bone tissue scaffolds, the colloidal stability of HA nanoparticles in solution is critical to obtain a uniform structure and desirable bulk properties [4–6]. In addition, HA-based composites crack under stress because of the brittle nature of HA [7]. To reinforce HA-based composites, stronger and more flexible constituents, such as natural nanofibers, are needed.

Bacterial cellulose (BC) nanofibers were chosen as a material to overcome the shortcomings of HA-based scaffolds due to their biocompatibility, potential to be used as a scaffold [8–11], and fibrous structure, with fiber diameters of several tens of nanometers, which is similar to that of collagen fibers [12,13]. 2,6,6-Tetramethylpiperidine-1-oxyl (TEMPO) radical oxidation is an easy method to obtain well-dispersed cellulose fibers without significant aggregation through the electrostatic repulsion of nanofibers [14], and oxidized cellulose nanofibers can effectively disperse nanomaterials [15,16].

In this study, we attempted to design a scaffold for bone tissue using nanofibrous TEMPO-oxidized BC (TOBC) as a structural framework and natural dispersant of HA nanoparticles. The colloidal stability of HA with TOBC and the mechanical properties of the scaffold were investigated. In addition, the unique properties of the composites, including physicochemical effects, viability, and differentiation of bone generating cells, were described.

2. Experimental

2.1. Materials

Gluconacetobacter xylinus (KCCM 40216) was obtained from the Korean Culture Center of Microorganisms. Calvarial osteoblasts isolated from the calvaria of neonatal (less than 1 day

* Corresponding author at: Department of Biosystems and Biomaterials Science and Engineering, Seoul National University, Seoul 151-921, Republic of Korea. Tel.: +82 28804624.
E-mail address: jhyun@snu.ac.kr (J. Hyun).

http://dx.doi.org/10.1016/j.colsurfb.2015.04.014
0927-7765/

old) Sprague–Dawley rats (SLC, Tokyo, Japan) via a digestive enzymatic process were provided from the lab of Prof. Byung-Soo Kim (Seoul National University, Seoul, Korea). Sodium hydroxide (≥98%) and D-mannitol (99%) were obtained from Samchun Chemicals (Korea). Yeast extract and bacto-peptone were purchased from BD (USA). 2,2,6,6-Tetramethylpiperidine-1-oxyl (TEMPO), NaBr, and NaClO were purchased from Sigma–Aldrich (USA). Hydroxyapatite (diameter >200 nm) nanoparticles, gelatin, and glutaraldehyde were purchased from Sigma–Aldrich. Phosphate buffered saline (PBS), Dulbecco's modified Eagle medium (DMEM), and fetal bovine serum (FBS) were purchased from Gibco (USA). Methylthiazolyldiphenyl tetrazolium bromide (MTT), ascorbic acid, β-glycerol phosphate, dexamethasone, Alizarin Red S, and cetylpyridinium chloride were purchased from Sigma–Aldrich. An ALP assay kit was purchased from Takara Bio (Japan).

2.2. Biosynthesis and purification of BC

The bacteria were cultured on mannitol media composed of 2.5% (w/w) mannitol, 0.5% (w/w) yeast extract, and 0.3% (w/w) bacto-peptone. Bacteria were introduced to Petri dishes containing culture medium at 28 °C for 5 days. After incubation, the BC membrane was harvested and purified with 1 wt% NaOH followed by washing with distilled water (DI water). The membrane was stored in DI water prior to use.

2.3. TEMPO-oxidation of BC

To obtain TEMPO-oxidized BC, hydrogels (20 g wetting weight) were cut into small pieces and then suspended in 500 ml of distilled water containing 20 mg of TEMPO and 0.5 g of NaBr. Subsequently, 15 ml of NaClO solution was added to the BC suspension to initiate oxidation while maintaining the system at pH 10 with NaOH. The mixture was vigorously agitated using a magnetic stirrer for 2 days at room temperature. The oxidation was quenched by adding ethanol to the suspension at the end of the reaction. The products were washed with DI water, collected by centrifugation (3×), and dialyzed with running DI water.

2.4. Preparation of HA–TOBC dispersions in an aqueous solution

HA nanoparticles (Sigma–Aldrich, diameter >200 nm) were dispersed in DI water using TOBC as a dispersant. HA nanoparticles (2.5, 5, and 10 mg) were dispersed in 10 ml of a TOBC (dry weight: 5 mg) suspension in DI water. The weight ratios of HA nanoparticles to TOBC were 1:2, 1:1, and 2:1. As a control, 5 mg of HA nanoparticles were dispersed in 10 ml of DI water without TOBC. All of the samples were contained in glass vials and were sonicated for 1 min and then stored at room temperature for 1 day.

2.5. Preparation of HA–TOBC-based scaffolds incorporating gelatin

Sixty milligrams of HA nanoparticles were dispersed in 12 ml of DI water containing 60 mg of TOBC under sonication. Subsequently, 30 or 60 mg of gelatin was added to the HA–TOBC suspension solution and stirred at 50 °C for 1 h. Next, 3 ml of the gelatin and HA–TOBC mixture was dropped into Petri dishes and cooled at 4 °C overnight. The gel form of the mixture was transferred to a freezer at −25 °C to solidify. After the cross-linking of the solidified gel mixture using 2.5% glutaraldehyde, the sample was freeze-dried for 48 h. A control sample without HA nanoparticles was prepared using the same method. Solidified HA–TOBC without gelatin was referred to as HA–TOBC–0Gel, samples containing a gelatin-to-TOBC of 0.5:1 (by weight) were referred to as TOBC–0.5Gel or HA–TOBC–0.5Gel, and samples containing a 1:1 ratio were referred to as TOBC–1Gel or HA–TOBC–1Gel.

2.6. Characterization of the composites

The chemical structures of BC and TOBC were characterized by Fourier transform infrared spectroscopy (FT-IR spectroscopy; Nicolet iS5, Thermo Scientific, USA) using 32 scans at a resolution of 8 cm^{-1} over the wavenumber range of 4000–600 cm^{-1}.

The morphologies of the samples were observed using field emission scanning electron microscopy (FE-SEM; SUPRA 55VP, Carl Zeiss, Germany) at an acceleration voltage of 2 kV. Transmission electron microscopy (TEM) images of HA and HA–TOBC dispersions were obtained using energy-filtering transmission electron microscopy (EF-TEM, LIBRA 120, Carl Zeiss, Germany) at an acceleration voltage of 200 kV.

The zeta potentials of HA, TOBC, and HA–TOBC dispersions were measured by dynamic light scattering (Zetasizer Nano, Malvern, UK). Samples were dispersed in DI water, and measurements were carried out at 20 °C with folded capillary cells. Three runs were performed and averaged for each sample.

The mechanical properties (tensile strength) of the samples were investigated using a universal testing machine (UTM; GB/LRX Plus, Lloyd, UK) fitted with a 500-N load cell at room temperature. The test specimens were rectangular, with a gauge length of 10 mm, a width of 5 mm, and a thickness of 0.5 mm. The Young's modulus was recorded at the maximum load.

The swelling ratio was measured by soaking the sample in a PBS solution at room temperature for 24 h. The samples were initially weighed (W_0). After soaking, excess water was removed from the sample surface with filter paper and the samples were reweighed (W). The swelling ratio (S) was calculated from the following equation: $S = (W - W_0)/W_0$.

2.7. Cell seeding on scaffolds

Calvarial osteoblasts that were isolated from the calvaria of neonatal (less than 1 day old) Sprague-Dawley rats (SLC, Tokyo, Japan) via a digestive enzymatic process were provided by the lab of Prof. Byung-Soo Kim (Seoul National University, Seoul, Korea). Cells were cultured in DMEM (high glucose) supplemented with 10% (V/V) FBS, 100 mM ascorbic acid, 10 mM β-glycerol phosphate, 100 nM dexamethasone, and 100 U/ml penicillin in a humidified 5% CO_2 incubator at 37 °C. To seed the cells on scaffolds, each scaffold was cut into circular discs (~15 mm in diameter), which were then sterilized in 70% ethanol for 30 min. The specimens were then placed in a 96-well plate and washed several times with DI water. Subsequently, the specimens were immersed in the incubation medium for 1 h. Osteoblasts from the cultures were trypsinized, and 1×10^4 cells were seeded on the sterilized scaffold specimens in 96-well plates. The medium was changed every other day, and the cultures were maintained at 37 °C.

2.8. Evaluation of cellular viability and proliferation

Cellular viability and proliferation were assayed using MTT. The medium was removed from the cell-culturing well plates, which were then washed with PBS. Scaffold samples or wells with cells were loaded with 20 μl of MTT (5 mg/ml in PBS) and 100 μl of medium for 2 min at 37 °C under 5% CO_2. The produced formazan crystals were dissolved in 100 μl of DMSO, and the absorbance of the suspension was measured at 570 nm using a plate reader. The empty wells of a tissue culture polystyrene (TCPS) plate were used as a positive control.

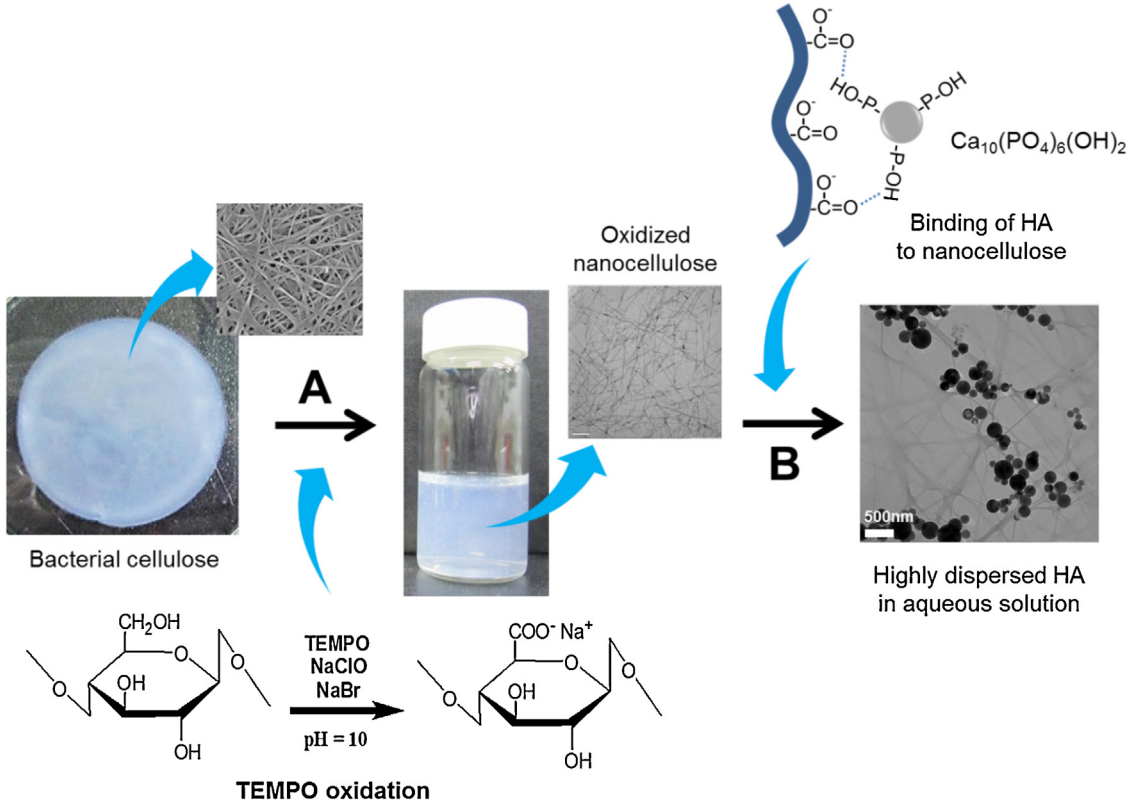

Fig. 1. Schematic diagram of the TEMPO-oxidation of BC and the colloidal dispersion of HA nanoparticles. (A) Negative charges are introduced to the surfaces of cellulose nanofibers after the TEMPO-oxidation of BC pellicles. The TEM image shows well-dispersed oxidized nanocellulose without aggregation in aqueous solution. (B) HA nanoparticles are bound to the surfaces of cellulose nanofibers by hydrogen bonding between the carboxyl groups of oxidized cellulose and the hydroxyl groups of HA.

2.9. Evaluation of cell differentiation and mineralization

The alkaline phosphatase (ALP) assay and Alizarin Red S staining were performed to observe cell differentiation and mineralization. The ALP of samples was extracted according to the ALP assay kit protocol, and absorbance was measured at 405 nm. For Alizarin Red S staining, the medium was removed from the well plates, and the wells were washed three times with PBS. The cells were fixed with 4% paraformaldehyde for 15 min at room temperature and then washed with DI water. The samples were incubated with 1% Alizarin Red S (Sigma–Aldrich) for 20 min at room temperature and then rinsed with DI water and methanol. The incorporated Alizarin Red S was extracted with 100 mmol/L cetylpyridinium chloride (Sigma–Aldrich) for 15 min at room temperature, and the absorbance at 562 nm was measured. The absorbance value of each sample was obtained by subtracting the absorbance of the blank material without cells from the absorbance of the material with cells. The empty wells of a TCPS plate were used as a positive control.

3. Results and discussion

3.1. Preparation and characterization of TOBC

Well-dispersed cellulose nanofibers were obtained by oxidizing BC with TEMPO. Primary hydroxyl groups at the C6 carbon of

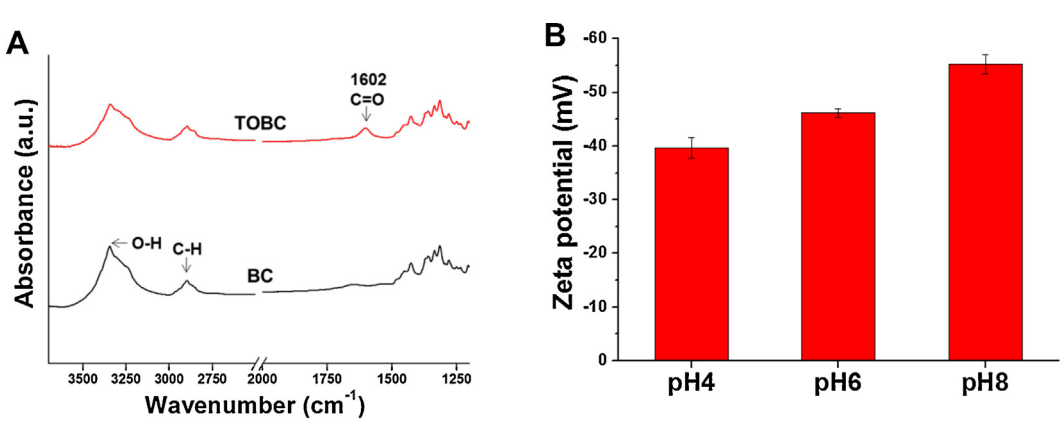

Fig. 2. Surface modification of cellulose nanofibers. (A) FTIR spectra of pure BC and TOBC. The formation of carboxyl groups in the presence of TOBC can be confirmed at 1602 cm^{-1}. (B) Zeta potentials of TOBC-dispersed solutions at different pH values. Data are the means ± standard deviations from three specimens.

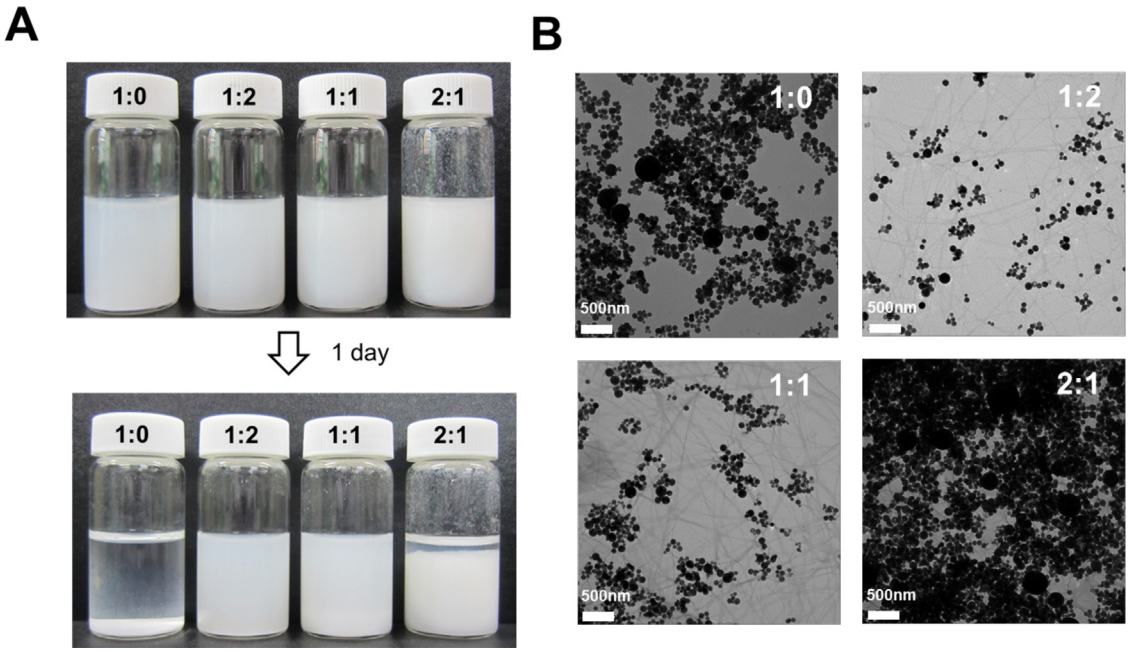

Fig. 3. Colloidal stability of HA nanoparticles and TOBC in DI water. (A) Images of HA nanoparticle/TOBC solutions with weight ratios of 1:0, 1:2, 1:1, and 2:1. (B) TEM images of HA nanoparticles dispersed along the TOBC nanofibers. HA nanoparticles were dispersed in aqueous solution containing TOBC at pH 8. The HA nanoparticle colloidal solution without TOBC showed rapid precipitation in 10 min (1:0), and excess HA nanoparticles resulted in severe aggregation (2:1). The specific adsorption of HA to the TOBC fibers and their well-dispersed state were confirmed in the HA–TOBC colloidal solutions with 1:2 and 1:1 ratios.

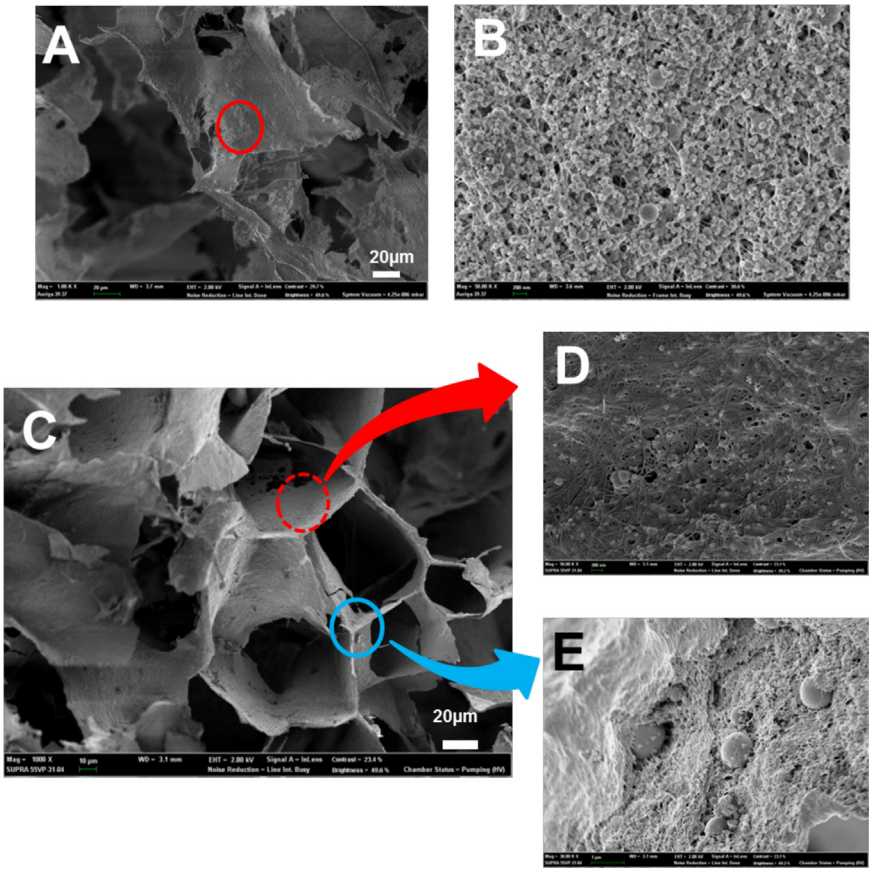

Fig. 4. FE-SEM micrographs of (A) HA–TOBC composite, (B) magnified images of the surface of the porous wall of HA–TOBC and (C) HA–TOBC–1Gel composite. Magnified images of (D) the porous wall surface (red dotted circle) and (E) cross section (blue solid circle) of the HA–TOBC–1Gel composite. (For interpretation of the references to color in this figure legend, the reader is referred to the web version of this article.)

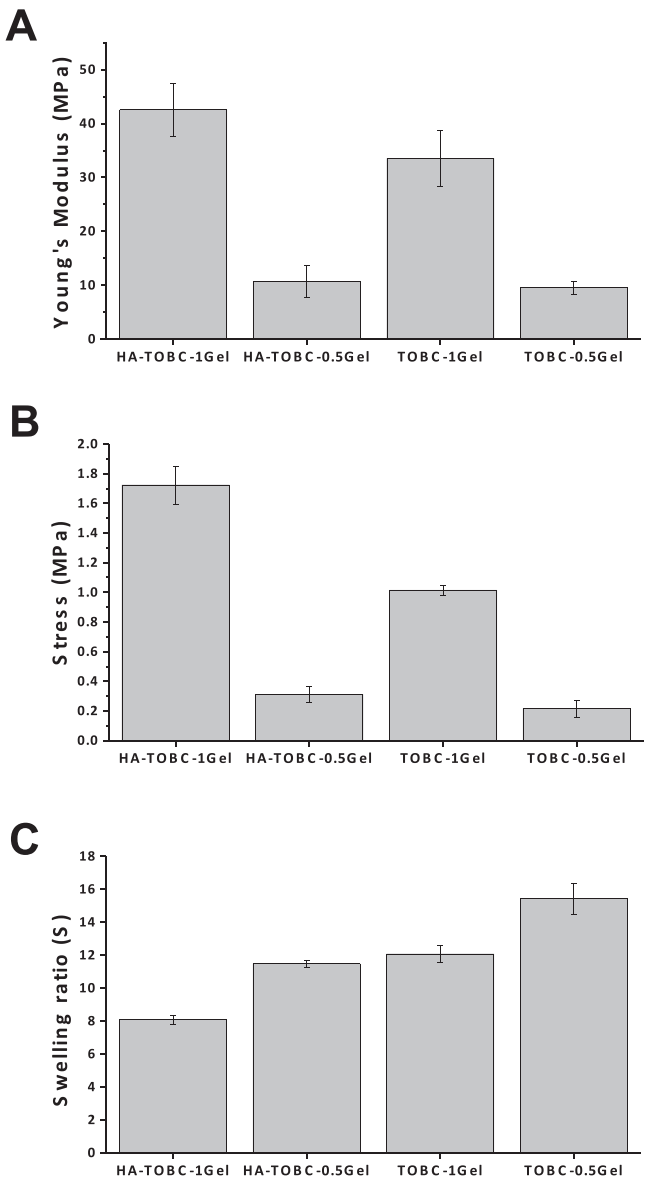

Fig. 5. Mechanical properties of composites: the (A) Young's modulus; (B) stress at the maximum load; and (C) swelling ratio. Data are the means ± standard deviations from ten specimens.

BC were converted to carboxylate groups by the oxidation reaction. TEMPO-mediated oxidation could occur regioselectively on the surface of cellulose fibrils because this reaction proceeded from regions that were accessible to the chemical solution [17]. Therefore, oxidized BC was able to maintain its original fibrous structure with a slightly decreased fiber length. Fig. 1 represents the process of preparing surface-modified cellulose nanofibers for dispersing HA nanoparticles. BC hydrogel contains more than 98% water, allowing it to react easily with oxidizing agents in aqueous solution. After oxidation, the highly interlaced fibers of pure BC swelled and dispersed in DI water due to the electrostatic repulsion among the negatively charged fiber surfaces. The well-dispersed TOBC nanofibers were confirmed by the EM images.

Fig. 2A shows the FT-IR spectra of BC and TOBC. The asymmetric stretching band of carboxyl groups at 1602 cm^{-1} in the TOBC spectrum confirmed that oxidation occurred. In addition, the stretching vibration bands of the C—H and —OH groups at 2896–2990 cm^{-1} and 3345–3539 cm^{-1}, respectively, were considerably reduced [18–20]. The equivalence point of TOBC was approximately pH 8, and its carboxyl group content, determined by titration, was 1.09 mmol/g.

The zeta potential values of TOBC at pH 4, 6, and 8 were −39.7 ± 2, −46.2 ± 0.8, and −55.3 ± 1.8 mV, respectively (Fig. 2B). TOBC fibers were unable to ionize completely at pH 4 because the pK_a value of the carboxyl groups is 3.5. The TOBC nanofibers were partially assembled, and the transparency of the dispersion solution was slightly less than that of the TOBC dispersion at pH 6. In contrast, according to the titration results, most of the carboxyl groups were ionized at pH values above 8. As a result, the aqueous dispersion of the TOBC at pH 8 had a better ability to disperse HA nanoparticles than the TOBC dispersions at pH 4 and 6. Once TEMPO-oxidized cellulose fibrils were well dispersed in solution, the stability of the dispersion solution was maintained for over 1 month.

3.2. Colloidal stability of HA–TOBC and the preparation of composites

The colloidal stability of HA nanoparticles in an aqueous solution is critical because of their strong tendency to aggregate. We evaluated the feasibility of TOBC nanofibers as a natural dispersant of HA nanoparticles. HA nanoparticles were dispersed in an aqueous solution containing TOBC at pH 8 to maintain the colloidal stability of the dispersion solution (Fig. 3A). TOBC has carboxyl groups that can participate in hydrogen bonding with P—OH in HA and carboxyl groups that can provide repulsive charges to maintain the stability of the colloidal dispersion. The HA nanoparticles were easily adsorbed on the surfaces of the TOBC fibers through hydrogen bonding, and the nanoparticles that dispersed in TOBC colloidal solutions at ratios of 1:2 and 1:1 maintained their colloidal stability even after 1 day of storage. However, the HA nanoparticle colloidal solution without TOBC showed rapid precipitation in 10 min, and excess HA nanoparticles exhibited severe aggregation, even with the addition of TOBC in solution, as observed in the 2:1 HA:TOBC sample (Fig. 3A).

Because BC pellicles form densely packed three-dimensional networks, it was difficult to obtain uniformly distributed BC nanofibers without chemical surface modification. To compare the colloidal stability of HA-untreated cellulose dispersions with HA–TOBC dispersions, microfibrillar cellulose (MFC) suspensions were obtained by homogenizing plant pulp. The MFC suspension mixed with HA nanoparticles at a 1:2 ratio was unstable and showed severe precipitation in 10 min (Supplementary Information).

The specific adsorption of HA to the TOBC fibers was confirmed by the TEM images (Fig. 3B). HA nanoparticles without TOBC aggregated nonspecifically, as shown in Fig. 3B. However, the HA–TOBC colloidal solutions at 1:2 and 1:1 ratios exhibited well-dispersed nanoparticles along the TOBC nanofibers. Meanwhile, the 2:1 HA–TOBC colloidal solution formed extensive aggregates of HA nanoparticles between the TOBC nanofibers due to the inherent adsorptive nature of the HA (Fig. 3B).

The HA nanoparticles without TOBC had a weak positive charge (4 mV) and interacted with the TOBC surface, which had a strong negative charge (−55 mV). The 1:1 HA–TOBC dispersions exhibited a charge of approximately −35 mV, representing an increase of approximately 20 units from the zeta potential of the TOBC dispersions at pH 8 due to the neutralization of the TOBC nanofiber surfaces by the HA nanoparticles. Normally, a zeta potential of ±30 mV is required to maintain a metastable suspension. The negative charge of HA–TOBC dispersions (−35 mV) was still strong enough to maintain colloidal stability in aqueous solution. In

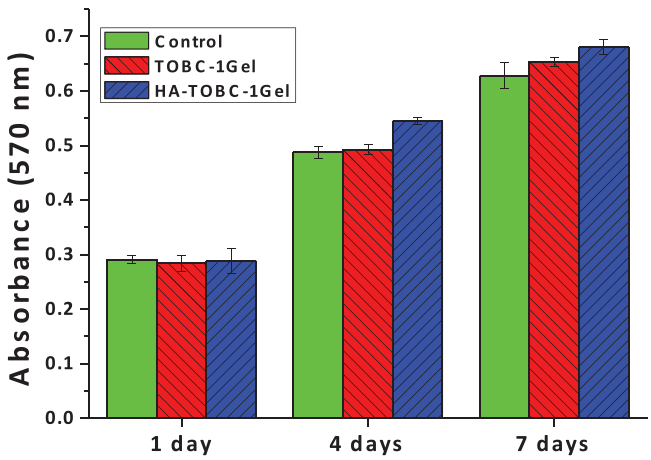

Fig. 6. Proliferation of cells by MTT assay on the TOBC–1Gel, HA–TOBC–1Gel, and TCP vs. time. Empty wells of a TCPS were used as a positive control. Data are means ± standard deviations from five specimens.

contrast, the zeta potential of 1:2 HA–MFC was −11 mV immediately after mixing, which was not sufficient to maintain the colloidal stability in solution, as indicated by the HA nanoparticles without TOBC.

3.3. Composite morphology

Three-dimensional interconnected porous structures are necessary to provide biofluidic pathways for the attachment, proliferation, and differentiation of cells. Well-dispersed HA–TOBC formed a highly porous structure without the incorporation of any porogens (Fig. 4A). HA nanoparticles in HA–TOBC were attached to the fiber surface at a high density (Fig. 4B). However, the pore shape was destroyed easily in solution due to the lack of binding forces. Gelatin was a perfect choice to satisfy the issue of the morphological stability because of the simple crosslinking chemistry for the formation of a gel state. In addition, gelatin is a collagen-derived biocompatible material that is essential for the enhancement of cell adhesion, proliferation, and differentiation in bone tissue engineering [21].

Because the isoelectric point of gelatin is pH 5, it is negatively charged at pH 8. The HA–TOBC–gelatin colloidal solution was well dispersed at 40 °C and changed into a gel at 4 °C (pH 8). After the chemical crosslinking of the HA–TOBC–gelatin colloidal solution at 4 °C with glutaraldehyde, it became a dimensionally stable gel, even at elevated temperatures greater than 40 °C.

Fig. 4C shows that the pore surface of the HA–TOBC–1Gel was composed of nanofibers decorated with HA nanoparticles, similar to HA–TOBC. However, the pore surfaces were smoother than in the HA–TOBC composite because the nanofibers were covered with a thin layer of gelatin. A rough micron-scale composite surface due to the aggregation of HA particles has been reported to retard the cell proliferation rate [22]. However, nanoscale roughness caused by well-dispersed HA nanoparticles could enhance cell attachment and proliferation. The cross-section of the thin gelatin layer was composed of densely packed cellulose nanofibers with numerous HA nanoparticles. This nanofibrous structure could significantly enhance the interaction between the scaffold and cells.

3.4. Mechanical and swelling properties of composites

Fig. 5A and B shows the Young's modulus and maximum tensile stress of the samples. The Young's moduli of HA–TOBC–1Gel,

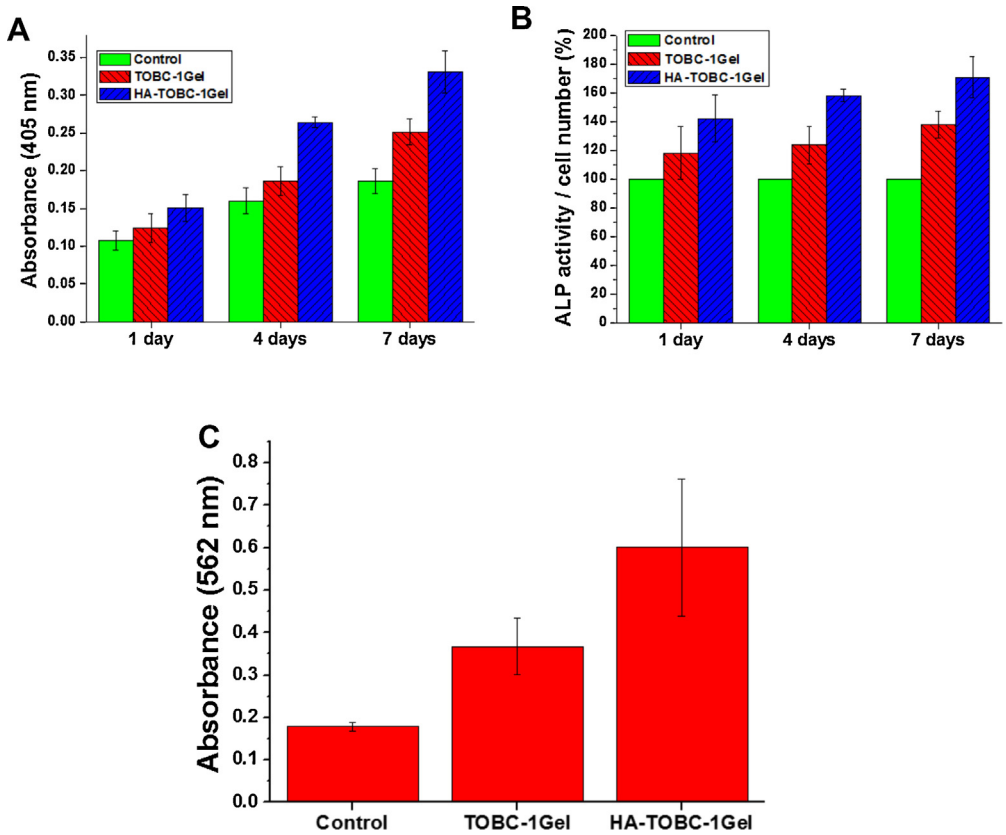

Fig. 7. Bioactivity of Calvarial osteoblasts cultured with gel composites. (A) ALP assay and (B) ALP activity of cells cultured on TOBC–1Gel, HA–TOBC–1Gel, and TCPS vs. time. (C) Quantification of mineral deposition in cells by Alizarin Red S staining on TOBC–1Gel, HA–TOBC–1Gel, and TCPS after 7 days of incubation. Empty wells of a TCPS were used as a positive control. Data are the means ± standard deviations from five specimens.

HA–TOBC–0.5Gel, TOBC–1Gel, and TOBC–0.5Gel were 42.5 ± 5.0, 11.2 ± 0.2, 12.6 ± 0.5, and 15.0 ± 0.9 MPa, respectively, while the corresponding maximum tensile stress values were 1.72 ± 0.13, 0.31 ± 0.06, 1.01 ± 0.03, and 0.22 ± 0.06 MPa, respectively. Both the Young's modulus and maximum tensile stress increased as the amount of gelatin increased. The enhanced mechanical properties of the composites resulted from the increased crosslinking of gelatin by glutaraldehyde as the amount of gelatin increased. In addition, the Young's modulus and maximum tensile stress increased with the addition of HA because the well-dispersed HA produced a denser scaffold structure.

The effects of the gelatin concentration and the presence of HA nanoparticles on the swelling ratios are demonstrated in Fig. 5C; the swelling ratios of HA–TOBC–1Gel, HA–TOBC–0.5Gel, TOBC–1Gel and TOBC–0.5Gel were 8.3 ± 0.3, 11.2 ± 0.2, 12.6 ± 0.5, and 15.0 ± 0.9, respectively. The swelling ratios illustrated that all samples had high water sorption capacities. However, the swelling ratio decreased with increasing gelatin concentration and with the addition of HA nanoparticles.

3.5. Proliferation of cells by MTT assay

Scaffolds should be non-cytotoxic and non-immunogenic and should be able to support cell attachment, proliferation, and differentiation. The cell viability and growth rate results indicated that the scaffolds made from TOBC–1Gel and HA–TOBC–1Gel were biocompatible and produced progressive cell growth. The number of cells on the tissue culture plates and scaffolds steadily increased with time for all of the samples. Cells on HA–TOBC–1Gel grew significantly and showed greater proliferation than other samples (Fig. 6).

3.6. ALP assay and Alizarin Red S staining

ALP staining and Alizarin Red S staining were performed to assess osteoblast differentiation and function, respectively (Fig. 7). Bone-type ALP contains membrane-bound glycoproteins and is commonly used as a marker of osteoblastic differentiation due to its ability to bind to the osteoblast membrane; it also enhances osteogenesis. Similar to the MTT assay results, the absorbance of ALP staining gradually increased with time for all samples (Fig. 7A). Interestingly, the HA–TOBC–1Gel scaffold showed significantly increased ALP staining. The ALP assay values were divided by the cell numbers and the control ALP assay value to show the increase in activity compared to the control. As shown in Fig. 7B, the HA–TOBC–1Gel scaffold showed the highest ALP activities on all days, and the difference was greatest at day 7.

Alizarin Red S was used to evaluate the relative value of calcium deposition. Cells were cultured on TOBC–1Gel, HA–TOBC–1Gel, and tissue culture plates (TCPs) as a control for 7 days. Alizarin Res S solution was then added to the samples. Alizarin Red S selectively bound to calcium salts and was then eluted by cetylpyridinium chloride to quantify calcium deposition. The amount of calcium deposition from cells cultured with the HA–TOBC–1Gel scaffold produced 3.38- and 1.64-fold greater levels of Alizarin Red S than those grown using TCP and the TOBC–1Gel scaffold, respectively (Fig. 7C). Therefore, more calcium was deposited on the HA–TOBC–1Gel scaffold.

The HA nanoparticles and cellulose nanofiber structure induced cell differentiation. The HA–TOBC–1Gel scaffold exhibited a greater ALP level and calcium deposition value, possibly due to the HA, which is widely known to accelerate mineralization. In addition, the structure of the cellulose nanofibers decorated with HA nanoparticles is similar to ECM, which had a positive effect on cell differentiation [22]. These results confirmed that the HA–TOBC–Gel composite could be applied for bone tissue scaffolds.

4. Conclusions

HA–TOBC–Gel composites were designed for application in bone tissue scaffolds. TEMPO-oxidized bacterial cellulose (TOBC) improved the colloidal stability of HA nanoparticles via the electrostatic repulsion between the fibers and the binding affinity of HA to TOBC. TOBC acted as a dispersion agent and a critical material of the composite gel structure, enhancing the mechanical properties of the HA–TOBC–Gel. Scaffolds prepared with HA–TOBC–Gel could be applied for osteoblastic cell proliferation and differentiation without cytotoxicity. The composite may be a promising candidate as a bone tissue-generating scaffold.

Acknowledgments

This research was supported by the Basic Science Research Program through the National Research Foundation of Korea (NRF), funded by the Ministry of Science, ICT and Future Planning (Grant Number 2014016093). The authors are grateful to Prof. Byung-Soo Kim in the School of Chemical and Biological Engineering, Seoul National University, for providing Calvarial osteoblasts.

Appendix A. Supplementary data

Supplementary data associated with this article can be found, in the online version, at http://dx.doi.org/10.1016/j.colsurfb.2015.04.014

References

[1] M.B. Yaylaoglu, P. Korkusuz, U. Ors, F. Korkusuz, V. Hasirci, Biomaterials 20 (1999) 711–719.
[2] H.W. Kim, J.C. Knowles, H.E. Kim, J. Biomed. Mater. Res. A 72A (2005) 136–145.
[3] P.A. Williamson, P.J. Blower, M.A. Green, Chem. Commun. 47 (2011) 1568–1570.
[4] H.W. Kim, H.E. Kim, V. Salih, Biomaterials 26 (2005) 5221–5230.
[5] H.J. Lee, H.W. Choi, K.J. Kim, S.C. Lee, Chem. Mater. 18 (2006) 5111–5118.
[6] C.F. Li, G.C. Li, S.G. Liu, J.H. Bai, A.J. Zhang, Colloid Surf. A 366 (2010) 27–33.
[7] Y. Han, K.W. Xu, J.A. Lu, J. Mater. Sci.: Mater. Med. 10 (1999) 243–248.
[8] M. Zaborowska, A. Bodin, H. Backdahl, J. Popp, A. Goldstein, P. Gatenholm, Acta Biomater. 6 (2010) 2540–2547.
[9] C. Brackmann, M. Zaborowska, J. Sundberg, P. Gatenholm, A. Enejder, Tissue Eng. Part C: Methods 18 (2012) 227–234.
[10] S.I. Jeong, J.O. Jeong, J.B. Choi, Y.M. Shin, J.S. Park, H.J. Gwon, Y.C. Nho, S.J. An, M.Y. Park, Y.M. Lim, Tissue Eng. Regen. Med. 11 (2014) 56–63.
[11] D. Ramani, T.P. Sastry, Cellulose 21 (2014) 3585–3595.
[12] N. Petersen, P. Gatenholm, Appl. Microbiol. Biotechnol. 91 (2011) 1277–1286.
[13] W.K. Czaja, D.J. Young, M. Kawecki, R.M. Brown, Biomacromolecules 8 (2007) 1–12.
[14] A. Isogai, T. Saito, H. Fukuzumi, Nanoscale 3 (2011) 71–85.
[15] H. Koga, T. Saito, T. Kitaoka, M. Nogi, K. Suganuma, A. Isogai, Biomacromolecules 14 (2013) 1160–1165.
[16] L. Valentini, M. Cardinali, E. Fortunati, L. Torre, J.M. Kenny, Mater. Lett. 105 (2013) 4–7.
[17] T. Saito, S. Kimura, Y. Nishiyama, A. Isogai, Biomacromolecules 8 (2007) 2485–2491.
[18] N. Lin, C. Bruzzese, A. Dufresne, ACS Appl. Mater. Interfaces 4 (2012) 4948–4959.
[19] S. Fujisawa, Y. Okita, H. Fukuzumi, T. Saito, A. Isogai, Carbohydr. Polym. 84 (2011) 579–583.
[20] H. Dong, J.F. Snyder, K.S. Williams, J.W. Andzelm, Biomacromolecules 14 (2013) 3338–3345.
[21] J.M. Zhu, R.E. Marchant, Expert Rev. Med. Devices 8 (2011) 607–626.
[22] H. Backdahl, G. Helenius, A. Bodin, U. Nannmark, B.R. Johansson, B. Risberg, P. Gatenholm, Biomaterials 27 (2006) 2141–2149.